Journal of Zhejiang University-SCIENCE A (Applied Physics & Engineering)
ISSN 1673-565X (Print); ISSN 1862-1775 (Online)
www.jzus.zju.edu.cn; www.springerlink.com
E-mail: jzus@zju.edu.cn

Longitudinal resistance performance of granular ballast beds under cyclic symmetric displacement loading*

Jie-ling XIAO[1,2], Hao LIU[†‡1,2], Jing-mang XU[1,2], Ping WANG[1,2], Gan-zhong LIU[1,2], Rong CHEN[1,2]

([1]*MOE Key Laboratory of High-speed Railway Engineering, Southwest Jiaotong University, Chengdu 610031, China*)

([2]*School of Civil Engineering, Southwest Jiaotong University, Chengdu 610031, China*)

[†]E-mail: liuhao@my.swjtu.edu.cn

Received Feb. 21, 2017; Revision accepted Apr. 24, 2017; Crosschecked July 7, 2017

Abstract: The longitudinal resistance performance of a granular ballast bed under cyclic symmetric displacement loading was studied based on a full-scale test model of ballast track structures. The change law of the longitudinal resistance characteristics of the ballast bed under variable displacement amplitudes was analyzed. The results show that: the resistance-displacement curves of a granular ballast bed are a set of closed hysteretic curves, indicating obvious energy consumption; a granular ballast bed softens gradually during the cyclic process with constant displacement amplitude, and the residual deformation rate increases nonlinearly with increasing cycle number; the peak value of the longitudinal resistance of lines decreases with increasing cycle number; the cyclic softening of a granular ballast bed is dependent on the displacement amplitude–the higher the displacement, the more severe the cyclic softening will become; after cyclic displacement loading is applied several times, the longitudinal resistance of the bed will degenerate obviously, and the higher the displacement amplitude, the higher the longitudinal resistance attenuation rate of the ballast bed will become.

Key words: Granular ballast bed; Displacement amplitude; Cyclic loading; Longitudinal resistance
http://dx.doi.org/10.1631/jzus.A1700058 **CLC number:** U213.71

1 Introduction

Granular ballast beds, characterized by structural dependence and discreteness, are solid and uneven structures constructed with crushed stone of different sizes according to a certain gradation. The mechanical properties of such beds are different from those of common solids or liquids because of the strong nonlinear bearing and shear resistance abilities, and generally they cannot directly withstand tension (Lim, 2004; Anderson and Fair, 2008; Han *et al*., 2015). Railway ballast bed structures have been adopted worldwide considering their good elasticity, excellent damping capacity, strong water permeability, and easy maintenance (Nurmikolu, 2012; Indraratna *et al*., 2014b). Continuously welded ballast tracks have become standard modern track structures (Esveld, 2001; Indraratna and Salim, 2005; Sung *et al*., 2005). The mechanical properties of ballast beds have been studied by many researchers. Hollow cylinder tests have been carried out to investigate the role of drainage conditions on the response of railway track foundation materials during cyclic loading (Mamou *et al*., 2017). The inclusion of geosynthetics and rubber mats for reducing the adverse effects of wheel loads was examined through an extensive field trial (Nimbalkar and Indraratna, 2016). In recent years, continuously welded rail track (CWR track)

‡ Corresponding author

* Project supported by the National Natural Science Foundation of China (Nos. 51425804, U1234201, and 1334203), and the Doctorial Innovation Fund of Southwest Jiaotong University (No. 2014310016), China

ORCID: Jie-ling XIAO, http://orcid.org/0000-0002-4692-7464; Hao LIU, http://orcid.org/0000-0002-6151-9805

technology has matured, and huge railway networks and complicated operating environments have brought tremendous pressure on the safe application of CWR tracks. The longitudinal resistance of ballast beds, which is closely related to line stability and rail creeping, is still an important issue for scientific research, especially the longitudinal resistance and distribution of bridge CWR section ballast beds, which directly influence bridge and rail design plans (Le Pen, 2008; Chen *et al*., 2013; Yan and Dai, 2014). The longitudinal load-bearing and force-transference mechanisms of ballast beds are very complicated because of the discreteness of the beds, the composition of track structures, the variety and cycles of load, and the dynamic performance of the live load effect. On the one hand, the stress performance of ballast beds is related to the loading course and displacement; on the other hand, granular ballast structures always change randomly and significantly (Indraratna *et al*., 2010). The longitudinal resistance of granular ballast beds has significant nonlinear characteristics. The displacement state and the force-displacement incremental relation reflecting the loading course dependency should be considered for the longitudinal resistance of lines under complicated stress states (Ruge and Birk, 2007). Longitudinal resistance testing has shown that after being stressed, ballast grains are transferred to a new and more stable equilibrium position (Kerokoski, 2010; Hayano *et al*., 2014; Le Pen *et al*., 2014; Zakeri and Barati, 2015). The structural response of granular ballast beds under longitudinal loading is closely related to the displacement amplitude. Because of the periodicity of temperature and the cyclic train load, ballast beds are always subject to dynamic changes from different displacement results. Since ballast grains are always subject to equilibrium-transfer-redistribution, the distribution of ballast bed resistance is characterized by discreteness, randomness, and strong nonlinearity.

Hence, the study of resistance performance and the change law of granular ballast beds under repeated longitudinal loading can be considered as a foundation for a deeper understanding of the dynamic service performance of ballast CWR tracks and of the stress deformation mechanism of CWR tracks under cyclic loading. The following is an analysis of the longitudinal resistance performance of a ballast bed under cyclic displacement loading and the influence of variable displacement loading amplitudes on the longitudinal resistance of the bed, conducted using a full-scale test model and a special loading system.

2 Test model and loading conditions

2.1 Model plan and scale

The meso-structure of granular ballast beds is complicated, and their mechanical properties can be significantly influenced by scale effects and gradation (Indraratna *et al.*, 2014a). Simulations relating to the gradation characteristics, contact relationships, and load-caused deformation of ballast grains performed using reduced models are limited to dimensional analysis and scale effects. Full-scale models are ideal for analysis (Kennedy, 2011). In addition, considering the complicated interaction between the track frame and the ballast bed of a CWR track under external loading, a full-scale track panel-ballast bed model selected as the test object is more applicable for simulating *on-site* ballast bed structures (Le Pen and Powrie, 2011). The number of sleepers in track frames is closely related to the resistance of the ballast bed, and does not greatly influence the change law of the resistance (Esveld, 2001; Indraratna and Salim, 2005). Therefore, a track panel with six sleepers was selected as the test model. The four sleepers in the middle were used as the test objects and the sleepers at each end were considered as the model boundaries. In addition, the displacement of the rail and each sleeper was tested. The results show that the sleeper displacement is almost the same as the rail displacement, which proves that the whole panel moves together.

2.2 Main technical parameters

The model track had a CHN60 rail, type-II fastener system, and type-III concrete sleepers with shoulders. The sleeper spacing was 0.6 m. The ballast bed was paved with class I materials. Before paving, the ballast particle sizes were classified with a standard square plug gauge to ensure the gradation of the formed ballast met code requirements (TB/T 2140-2008) (MOR, 2008). The ballast material was crushed basalt stone. The gradation in ballast particle size is shown in Fig. 1. The Los Angeles abrasion rate (LAA) of the ballast particles was 23%. The standard aggregate impact toughness (IP) was 97%, the

marked aggregate crushing rate (CA) was 8%, and the ballast aggregate crushing rate (CB) was 20%. The compressive strength of the stone powder test was 0.3 MPa.

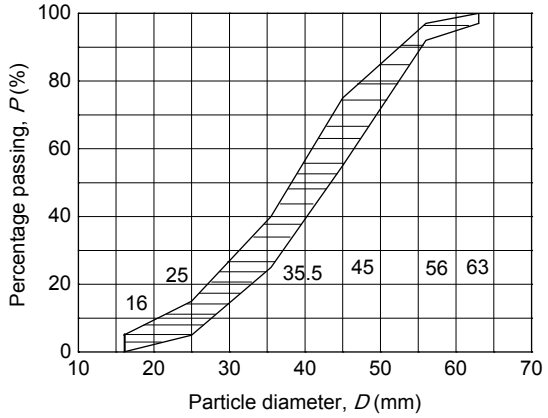

Fig. 1 Gradation of ballast particle size

The section size of the ballast bed met the requirements for single line ballast beds of a 350 km/h ballast track. The top width was 3.60 m and the thickness 0.35 m. The slope of the ballast shoulder was 1:1.75. The piled ballast shoulder was 0.15 m. The top of the ballast bed was 40 mm lower than the rail support surface of the sleepers (Jing, 2012; Wang *et al*., 2015) (Fig. 2).

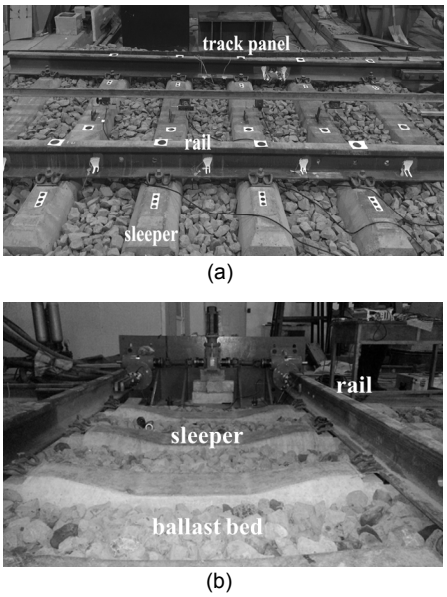

Fig. 2 Test model of the ballast bed
(a) Model track panel; (b) Model ballast bed

2.3 Loading apparatus

The model was equipped with a special loading apparatus consisting of an actuator unit, a sensor unit, and a data collection unit. The CF-300 kN precision power servo actuator, provided with a force or displacement control function, was used as the actuator unit for performing the two-way synchronization control test and controlling feedback through a servo drive system (Fig. 3). The sensor unit consisted of a spoke-type tension/pressure sensor (range: ±300 kN; accuracy: 0.01 kN) and a displacement transducer (range: ±50 mm; accuracy: 0.01 mm). A DHDAS dynamic signal analyzer was used as the data collection unit for realizing real-time collection and recording.

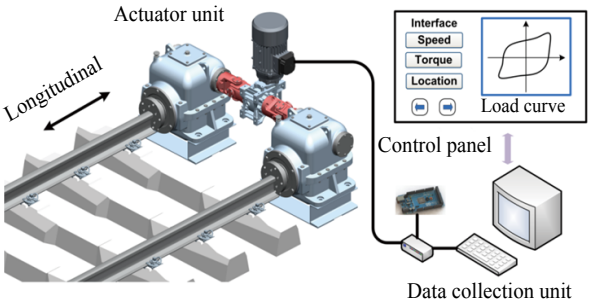

Fig. 3 Schematic diagram of the test apparatus

The actuator unit of the loading apparatus used for the test loaded the track frame synchronously through the two rails. The sensor unit and data collection unit were used for collecting and recording the measured load and displacement values of the track panel. The cyclic displacement or force load output of the actuator unit could be realized through the servo-feedback system and control center to simulate the stressed track panel under cyclic loading (Fig. 4) for estimating the longitudinal resistance of the ballast bed.

2.4 Test conditions

Granular ballast beds are always subject to much granule contact and slippage, and therefore feature viscoplasticity. The deformation characteristics under external loading are related to displacement (Zhou, 1995). To analyze the influence of cyclic symmetric displacement loading on the longitudinal resistance

of a ballast bed under variable displacement amplitudes, we conducted a study on a full-scale model through a loading apparatus. Temperature load is one of the main loads on CWR tracks, and its periodicity can subject ballast within sleeper cribs to cyclic "compression-loosening" changes which accordingly change the degree of compaction and the longitudinal resistance of a ballast bed. Therefore, several cyclic displacement amplitude loading plans, namely low displacement amplitude (4 mm, 6 mm), medium displacement amplitude (8 mm, 10 mm), and high displacement amplitude (20 mm), were designed and adopted for the test. In addition, to simulate the slow change process of temperature load and ensure the stability of the load, cyclic triangular loading was adopted (Zhou, 1995; Ruge and Birk, 2007). The loading rate was constant during cyclic triangular wave loading and therefore the change law of the longitudinal resistance could be analyzed when the displacement (u) amplitude was changed to low, medium or high. The loading curve is shown in Fig. 5.

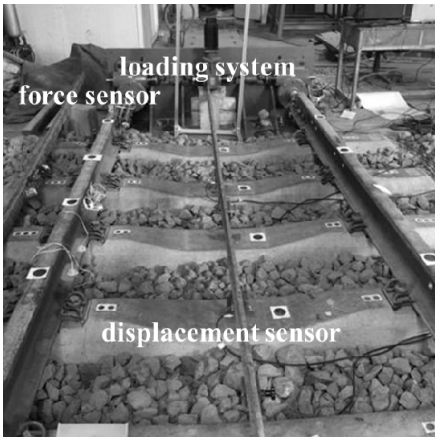

Fig. 4 Test of ballast bed longitudinal resistance

3 Ballast bed longitudinal resistance under cyclic symmetric displacement

The resistance of the ballast bed under variable displacement amplitudes during test loading was subject to obvious discreteness and nonlinearity. The dynamic changes were closely related to the displacement amplitude. The longitudinal resistance-displacement hysteretic curves of the ballast bed under cyclic symmetric single-axis displacement loading and variable displacement amplitudes are described below.

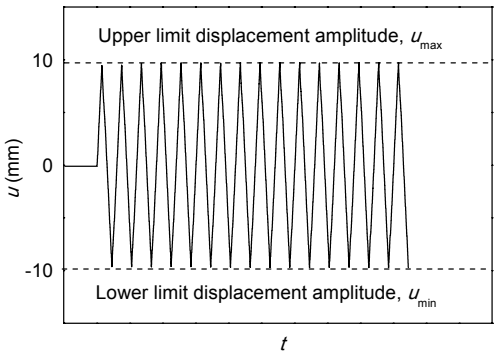

Fig. 5 Symmetric displacement cyclic load curve

3.1 Low displacement amplitude

The force-displacement curves of the granular ballast bed under cyclic loading formed a set of closed and relatively stable hysteretic curves (Fig. 6), indicating that the ballast bed was subject to a stable energy consumption state under longitudinal cyclic symmetric loading. The force-displacement curves obtained during initial loading showed a change coinciding with those obtained during unidirectional loading and did not coincide with the subsequent curve changes. For the subsequent cycle, the force-displacement curves were similar to each other, and the resistance of the ballast bed was subject to a stable hysteretic change.

To further analyze the influence of a low displacement amplitude loading cycle on the resistance and deformation of the ballast bed, curves reflecting the longitudinal ultimate resistance and residual plastic deformation (Fig. 6) were adopted. Curves relating these to the cycle number are shown in Fig. 7, where F_a refers to the longitudinal ultimate resistance, U_p refers to the ratio of the residual deformation to the unloading point displacement, and N_x refers to the number of loading cycles.

The residual deformation rate increased nonlinearly with increasing cycle number. The most rapid increase occurred during the first three cycles, and then it gradually became stable. The longitudinal ultimate resistance decreased with increasing cycle number. The most rapid decrease occurred during the

first two cycles, and then it attenuated slightly before finally stabilizing. When the displacement amplitude did not change during cycling, the longitudinal ultimate resistance decreased slightly with increasing cycle number. This can be considered a specific manifestation of granular ballast bed cyclic softening behavior in cyclic symmetric loading conditions. However, the cyclic softening was not obvious under low cyclic displacement loading, and the granular ballast bed tended towards stable cycling. The longitudinal ultimate resistance of the ballast bed decreased by about 10% when the displacement amplitude was 4 mm and the load was exerted 10 times. It decreased by about 16% when the displacement amplitude was 6 mm. Hence, when the longitudinal displacement amplitude is 6 mm or lower, the longitudinal resistance of the ballast bed was basically stable.

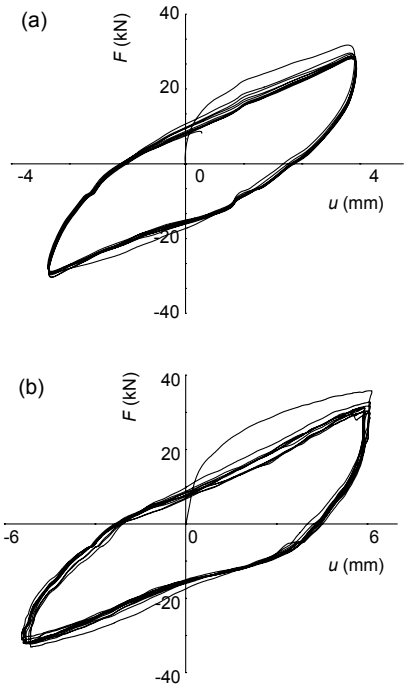

Fig. 6 Resistance-displacement curve under low cyclic displacement amplitude
(a) Displacement amplitude: 4 mm; (b) Displacement amplitude: 6 mm. *F* refers to the ballast longitudinal resistance

3.2 Medium displacement amplitude

The longitudinal resistance-displacement response curves obtained under medium displacement amplitudes are shown in Fig. 8.

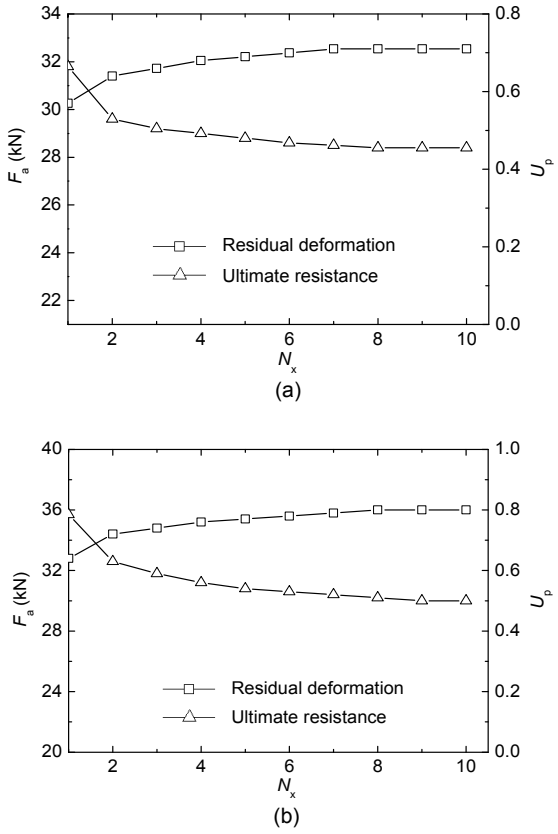

Fig. 7 Relationship between residual deformation, ultimate resistance, and cycle number
(a) Displacement amplitude: 4 mm; (b) Displacement amplitude: 6 mm

Taking the medium displacement amplitudes of 8 mm and 10 mm as examples, the residual plastic deformation and ultimate resistance in relation to the curves obtained under forward loading (Fig. 8) were adopted, and the curves relating these to the cycle number are shown in Fig. 9.

The loading and unloading curves obtained under cyclic loading displacement amplitudes of 8 mm and 10 mm also formed closed hysteretic curves. Compared with the test results obtained under low displacement amplitudes, the repeatability of the hysteretic curves was relatively unstable from the second loading cycle. A rapid increase of the residual plastic deformation rate occurred during the first five cycles, and a rapid decrease of the longitudinal ultimate resistance occurred during the first four cycles (Fig. 9). The cyclic softening behavior of the granular ballast bed was more obvious compared with that obtained under low displacement amplitudes. The

longitudinal ultimate resistance of the ballast bed decreased by about 20% after the load was exerted 10 times.

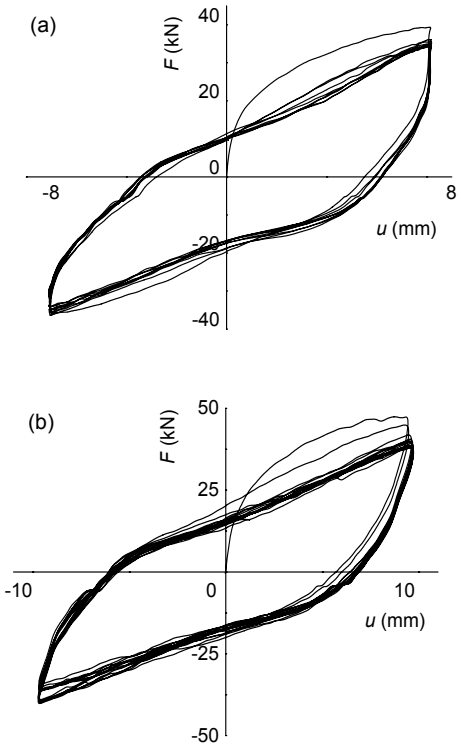

Fig. 8 Resistance-displacement curves under medium cyclic displacement amplitude
(a) Displacement amplitude: 8 mm; (b) Displacement amplitude: 10 mm

3.3 High displacement amplitude

In sections with high line creeping, the longitudinal displacement of a ballast bed can be far higher than 10 mm (UIC, 2001; Ruge and Birk, 2007). Therefore, the longitudinal resistance displacement curves of the ballast bed were tested under the high displacement amplitude conditions of ±20 mm displacement. The test results are shown in Figs. 10 and 11.

According to the test, when the displacement amplitude was relatively high, the granular ballast bed was subject to very obvious cyclic softening. Since the ballast bed was greatly disturbed, causing plastic flow of the ballast grains, the residual plastic deformation rate increased rapidly with increasing cycle number and was maintained at a high level. The ultimate resistance amplitude of the ballast bed attenuated quickly during the first five loading cycles before

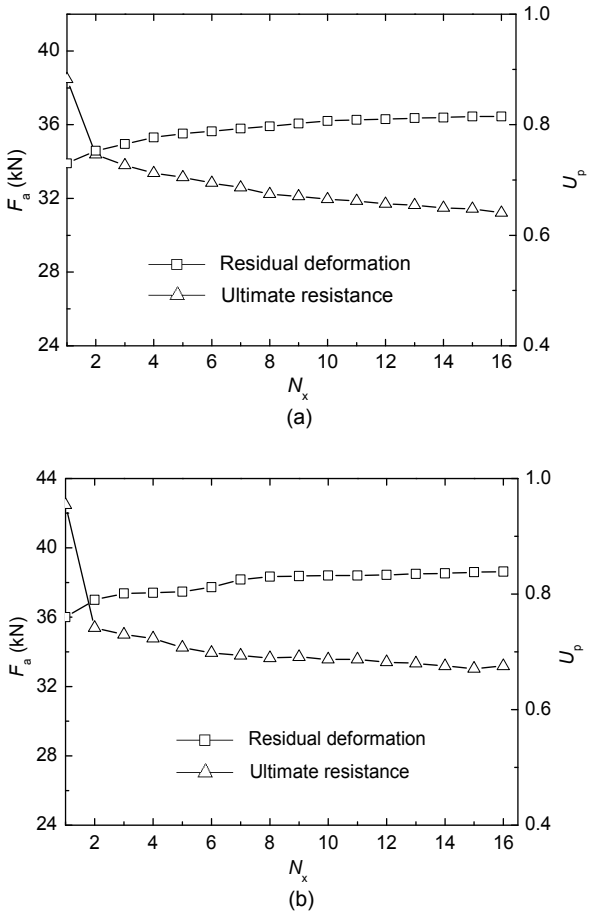

Fig. 9 Relationship between medium displacement amplitude response resistance and cycle number
(a) Displacement amplitude: 8 mm; (b) Displacement amplitude: 10 mm

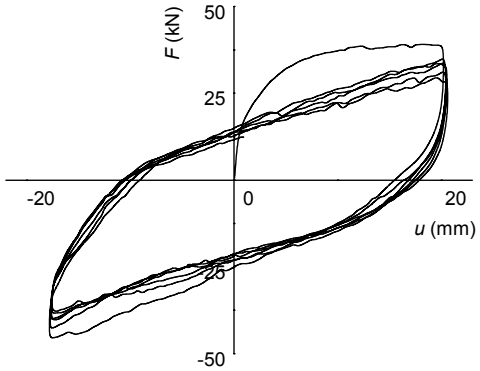

Fig. 10 Resistance-displacement curves under high cyclic displacement amplitude

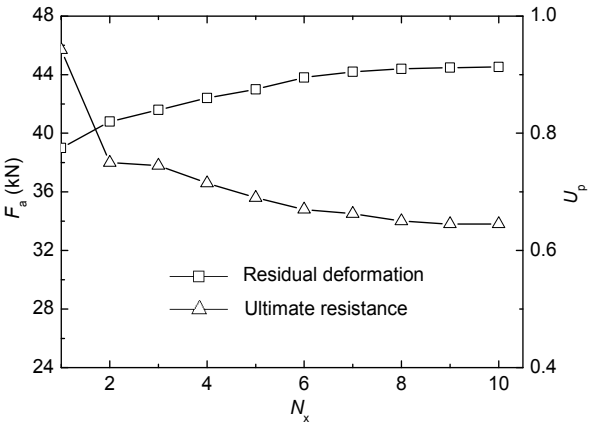

Fig. 11 Relationship between response resistance and cycle number

finally stabilizing. The longitudinal ultimate resistance of the ballast bed decreased by about 26% after the load was exerted 10 times. Hence, for the stress-induced deformation of ballast CWR tracks, especially CWR tracks on bridges with a large temperature span at the end of the bridge beam, the softening effect of resistance-displacement curves of the ballast bed obtained under repeated longitudinal displacement amplitudes at sections and subareas is of practical significance.

4 Hysteretic model of a granular ballast bed under cyclic displacement loading

4.1 Hysteretic model curve

When a component or a structure deforms due to an external force, the resistance restoring the initial state is called the restoring force. The deformation-restoring force interaction curve is called a hysteretic curve. For the tests in this study, the dynamic changes represented a cyclic loading behavior. A hysteretic model can be established according to the test curves of a cyclic load exerted on a granular ballast bed and used to obtain the longitudinal bearing and force transference capacities of granular ballast beds.

Hysteretic models used under cyclic loading, nominally, can be divided into linear models and continuously smooth curve models. At present, the longitudinal resistance model of lines used for CWR track calculation and analysis is a mathematical model obtained from resistance-displacement curves recorded during tests. This model can be simplified as a bilinear model (Chen *et al.*, 2013; Yan and Dai, 2014), reflecting the ideal elastic-plastic variation characteristics of a granular ballast bed. Fig. 12 shows the longitudinal resistance restoring force model for rail lines. The parameters of the model are the same as those of the resistance-displacement curves obtained under unidirectional loading. The bilinear model is dependent on the initial elastic stiffness and yield stiffness, so it is easy to use but cannot reflect characteristics such as the randomness and strong nonlinearity related to a granular ballast bed and the loading course. In addition, it has discontinuity points. The stiffness of the hysteretic curve model changes continuously (Fig. 13). Hysteretic models include index, power function, spline curve, and polynomial types, which more accurately describe the nonlinearity of non-resistance.

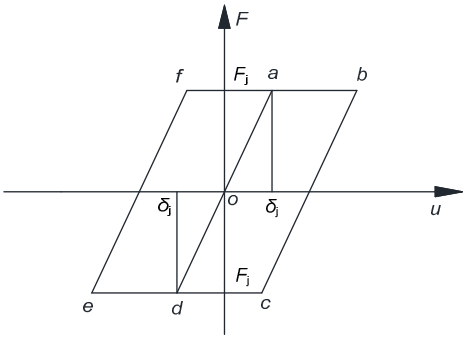

Fig. 12 Bilinear hysteretic model

F_j refers to the yield displacement, and δ_j refers to the yield resistance

4.2 Hysteretic rule

For monotonic loading curves of a granular ballast bed, a three-phase secondary yielding model can be used. The first, second, and third phases relate to elasticity, plastic hardening, and yielding, respectively. Quadratic parabolas can be used to describe the plastic hardening phase. The monotonic loading curve forms for different phases can be expressed as

$$F=\begin{cases}E_s u, & 0\le u\le u_s,\\ F_s+\dfrac{E_s(k_2-1)}{u_s k_1^2}(u-k_1u_s)^2, & u_s<u\le k_1u_s,\\ k_2F_s, & u>k_1u_s,\end{cases} \quad (1)$$

where E_s refers to the initial elastic stiffness, F_s refers to the plastic hardening resistance, u_s refers to the plastic hardening displacement, and k_1 and k_2 refer to the parameters for controlling the shapes of curves, which change with the strong nonlinearity of a granular ballast bed measured under variable stresses and can be adopted according to the test results.

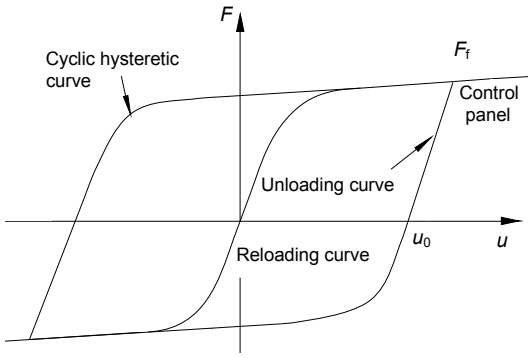

Fig. 13 Continuously smooth hysteretic curve model
F_f refers to the resistance at the peak point of the reloading curve, and u_0 refers to the displacement at the end of the unloading curve

Referring to the well-known Masing's rules (Hayashikawa *et al.*, 2004; Shi *et al.*, 2011), hysteretic curves/models were proposed to represent the ballast longitudinal resistance performance. The shape of the hysteretic curves was basically the same as those based on Masing's rules. However, in consideration of its discreteness and composition, the longitudinal resistance of a granular ballast bed has significant nonlinear characteristics. Thus, the parameters used for the skeleton curve and family of ballast hysteretic curves/models determined by different test conditions were different from those based on Masing's rules. The hysteretic curves of a granular ballast bed can be divided into loading, unloading, reloading, unloading, and reloading curves. When a load is exerted for the first time, the granular structure will be subject to longitudinal compression along the monotonic loading curve. If degeneration is neglected, the unloading, unloading stiffness, and initial elastic stiffness of the unloading curve are the same, according to the elastic sections. The unloading stiffness is the same as the initial elastic stiffness. The reloading curve reflects the track between the end of the unloading curve and the peak point of inverse direction loading (Fig. 14).

During hysteretic cycling, if stiffness degeneration is neglected, then $d_1=E_s(u-u_0)$, $d_2=(E_s-E_k)\times(u-u_0)$, and $E_k=(F_f-F_0)/(u_f-u_0)$ (Fig. 14), where E_k refers to the secant stiffness, F_0 refers to the resistance at the end of the unloading curve, and u_f refers to the displacement at the peak point of the reloading curve. The longitudinal bearing capacity of the ballast bed on a reloading curve can be calculated according to

$$F = E_s(u-u_0) + F_0 - (E_s - E_k)(u-u_0)k, \qquad (2)$$

where k refers to the proportionality coefficient, which can be obtained according to the test.

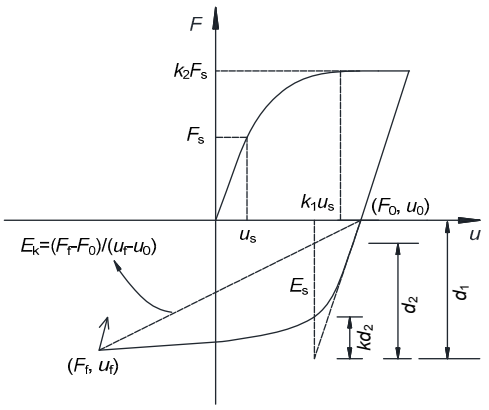

Fig. 14 Hysteretic rule of granular ballast beds under cyclic loading

4.3 Evolution of hysteretic curves of a granular ballast bed under cyclic displacement loading

For a granular ballast bed under cyclic displacement longitudinal loading, after being stressed, ballast grains will be transferred to a new and more stable equilibrium position. Cyclic densification takes place without much additional breakage due to the rearrangement of ballast particles (Indraratna *et al.*, 2010). This will affect the transference capacity of ballast longitudinal force and the hysteretic rules of the ballast layer. The dynamic displacement caused by longitudinal excitation causes a changing repeated cyclic hysteretic state in ballast bed resistance. This dynamic resistance is related to the degree of compaction of the ballast bed, the ballast material, and the dynamic displacement frequency and amplitude. At this time, the key problem for theoretical calculation to solve is the selection of an applicable hysteretic curve of dynamic resistance of the ballast bed.

Considering that the longitudinal resistance of sleepers is an important parameter for realizing stable lines, preventing rail creeping, and improving the temperature force homogeneity of long CWR tracks, the rail temperature force distribution can help to control the operation under a certain temperature condition (no-load) when designing CWR tracks. Hence, the influence of displacement amplitude measured under no-load conditions on the longitudinal resistance of a ballast bed is explored in this study. According to the above test results, when the cyclic displacement amplitude is constant, granular ballast beds will show cyclic degeneration, including longitudinal bearing capacity degeneration and residual deformation deterioration (Fig. 15).

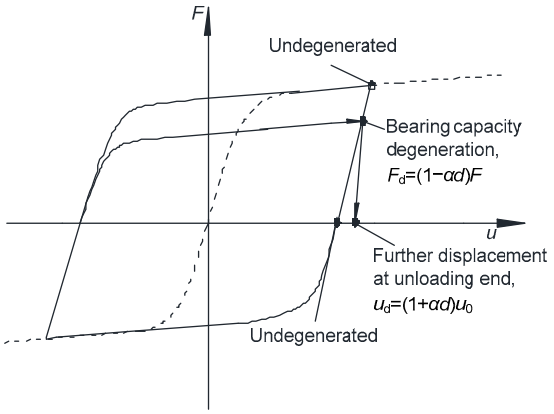

Fig. 15 Bearing capacity degeneration of granular ballast beds

F_d refers to the degenerated resistance at the peak point of the reloading curve, u_d refers to the degenerated displacement at the end of the unloading curve, α refers to the proportionality coefficient, and d refers to the degradation coefficient

The bearing capacity degeneration of the granular ballast bed equivalent constitutive model comprises mainly the ultimate resistance direction point degeneration during positive and inverse direction loading, i.e., the reduction of the last ultimate value during unloading after the displacement reaches the ultimate value. The residual deformation increase of the degeneration refers to the residual deformation at the end of the unloading curve (the start point of the reloading curve), during reloading, relative to the last residual deformation value.

Taking the bearing capacity degeneration as an example, suppose the defined resistance yielding function is φ_n:

$$\varphi_n = \frac{F}{F_{p,n-1}}. \tag{3}$$

Then the displacement yielding function will be ε_n:

$$\varepsilon_n = \frac{u}{u_{p,n-1}}. \tag{4}$$

In Eqs. (3) and (4), $F_{p,n-1}$ and $u_{p,n-1}$ refer to the yielding force and the corresponding displacement, respectively, under the load applied at the last step. Under cyclic loading, $\varphi_{s,n}$ and $\varphi_{s,n+1}$ refer to the initial yield functions of resistance of a member when loaded for the nth and $(n+1)$th times, and $\varphi_{p,n}$ and $\varphi_{p,n+1}$ refer to the absolute yield function of resistance when loaded for the nth and $(n+1)$th times, respectively. $\varphi_{u,n}$ refers to the yield functions of resistance when unloaded for the nth time. Because of the degeneration effect on the bearing capacity, $\varphi_{u,n}<\varphi_{u,n+1}$.

4.4 Degeneration of the granular ballast bed measured under cyclic displacement amplitude loading

The degeneration of a granular ballast bed under cyclic displacement amplitude loading is caused mainly by stressed and deformed grains. Hence, based on particle image velocimetry (PIV) image identification technology, the motion law of ballast grains under longitudinal displacement of track frames was analyzed (Fig. 16).

The test showed that when the sleepers move along in the longitudinal direction, the grains will show an irregular motion law. After loading, ballast grains will scatter and finally be transferred to a new equilibrium position. The higher the cyclic displacement amplitude, the more obvious the disturbance to the ballast bed is, and the more obvious the irregularity of the displacement and motion of the ballast grains will become. Fig. 17 shows the condition of the ballast grains examined under different displacement amplitudes. Arrows indicate movement after being loaded 10 times compared with the initial ballast bed state before loading.

The ballast bed is subject to a relatively stable energy consumption state under longitudinal cyclic loading when the displacement amplitude is low. Compared with the initial loading state, the ballast

grains will move slightly after a certain number of cycles. However, under a high displacement amplitude, the positions of the ballast grains change obviously, and the ballast bed gradually loosens and is subject to apparent cyclic softening.

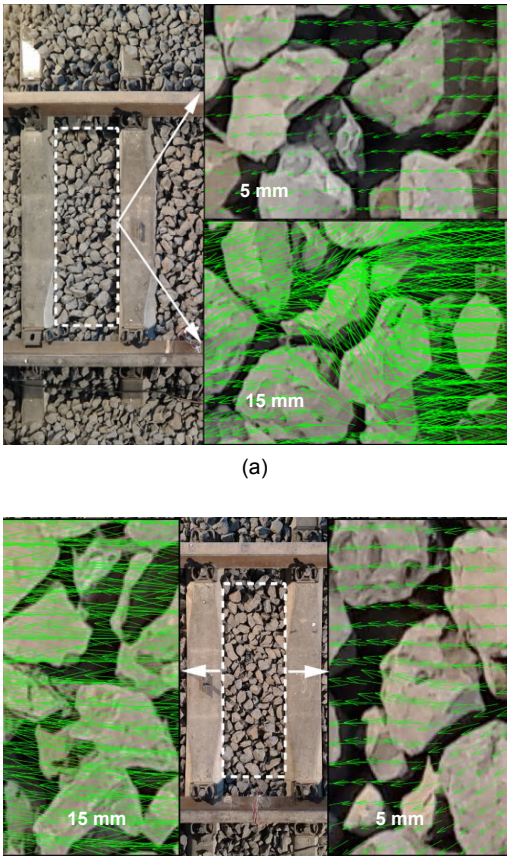

Fig. 16 Motion law of ballast grains under different sleeper displacements
(a) End of track panel; (b) Middle of track panel

From the test results of the longitudinal characteristics of the granular ballast bed obtained under different symmetric displacement amplitudes mentioned above, when the symmetric displacement amplitude increases, the ultimate longitudinal bearing capacity of the ballast bed will decrease, indicating a certain relation between them. The relation between the longitudinal resistance and cyclic displacement amplitudes of the ballast bed is shown in Fig. 18.

Displacement amplitudes influence the longitudinal resistance performance of the ballast bed greatly under cyclic loading. The longitudinal resistance of the ballast bed shows an obvious degeneration effect. Within the loading cycles for the test, the resistance attenuation rates of the ballast bed were 6%, 11%, and 18%, respectively. When the displacement amplitude was low, the longitudinal resistance of the ballast bed degenerated quickly within the first 10 loading cycles

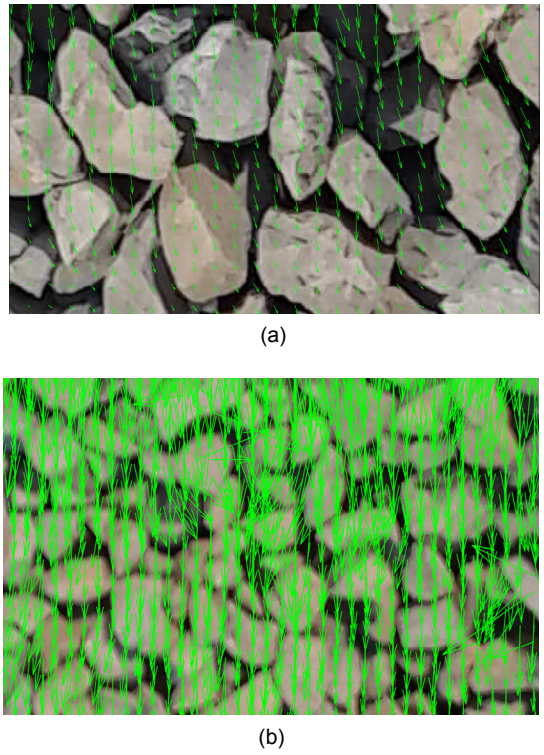

Fig. 17 Ballast steady state after 10 cycles
(a) Displacement amplitude: 4 mm; (b) Displacement amplitude: 10 mm

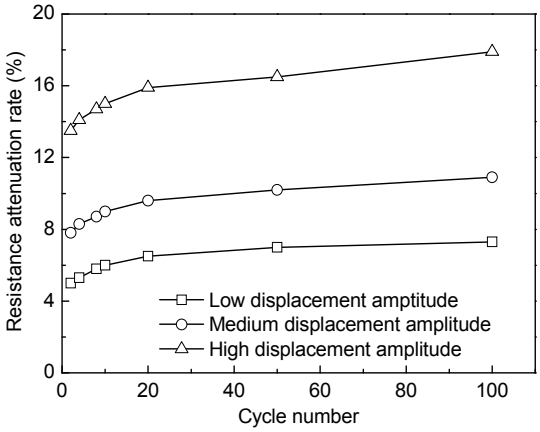

Fig. 18 Attenuation rate of ballast resistance under different displacement amplitudes

and then gradually stabilized. When the displacement amplitude was high, the cyclic softening rate decreased with increasing cycle number. But within the cycle number specified for the test in this study, the saturation effect of the cyclic softening behavior was inconspicuous, i.e., the longitudinal resistance of the ballast bed decreased continuously with increasing cycle number.

5 Conclusions

According to the test results, the following can be concluded:

1. The resistance-displacement curve of a granular ballast bed is a closed hysteretic curve under cyclic symmetric displacement amplitude loading, indicating obvious energy consumption.

2. When the displacement amplitude is constant, a granular ballast bed will show cyclic softening. For a ballast bed subject to durable dynamic reciprocated changes, the transference capacity of ballast longitudinal force is directly dependent on displacement amplitudes. After the cyclic displacement loading is exerted several times, the longitudinal resistance of the ballast beds will degenerate obviously.

3. The attenuation rate of the longitudinal resistance of a ballast bed changes with displacement amplitudes. The higher the displacement, the more apparent the degeneration effect will become. For some special CWR track sections, the decrease of resistance caused by a change of ballast bed conditions under high cyclic displacement loading should be given appropriate consideration.

References

Anderson, W.F., Fair, P., 2008. Behaviour of railroad ballast under monotonic and cyclic loading. *Journal of Geotechnical and Geoenvironmental Engineering*, **134**(3): 316-327. https://doi.org/10.1061/(asce)1090-0241(2008)134:3(316)

Chen, R., Wang, P., Wei, X.K., 2013. Track-bridge longitudinal interaction of continuous welded rails on arch bridge. *Mathematical Problems in Engineering*, **2013**:494137. http://dx.doi.org/10.1155/2013/494137

Esveld, C., 2001. Modern Railway Track. MRT Press, the Netherlands.

Han, J., Zhao, G.T., Xiao, X.B., *et al*., 2015. Effect of softening of cement asphalt mortar on vehicle operation safety and track dynamics. *Journal of Zhejiang University-SCIENCE A (Applied Physics & Engineering)*, **16**(12): 976-986. http://dx.doi.org/10.1631/jzus.A1500080

Hayano, K., Koike, Y., Nakamura, T., *et al*., 2014. Effects of sleeper shape on lateral resistance of railway ballasted tracks. Proceedings of the Geo-Shanghai International Conference, p.491-499. http://dx.doi.org/10.1061/9780784413425.050

Hayashikawa, T., Abdel Raheem, S.E., Hashimoto, I., 2004. Nonlinear seismic response of soil-foundation-structure interaction model of cable-stayed bridges tower. 13th World Conference on Earthquake Engineering, No. 3045.

Indraratna, B., Salim, W., 2005. Mechanics of Ballasted Rail Tracks: a Geotechnical Perspective. Taylor and Francis/ Balkema, London, UK.

Indraratna, B., Thakur, P.K., Vinod, J.S., 2010. Experimental and numerical study of railway ballast behavior under cyclic loading. *International Journal of Geomechanics*, **10**(4):136-144. http://dx.doi.org/10.1061/(asce)GM.1943-5622.0000055

Indraratna, B., Nimbalkar, S., Neville, T., 2014a. Performance assessment of reinforced ballasted rail track. *Proceedings of the Institution of Civil Engineers-Ground Improvement*, **167**(1):24-34. http://dx.doi.org/10.1680/grim.13.00018

Indraratna, B., Nimbalkar, S., Rujikiatkamjorn, C., 2014b. From theory to practice in track geomechanics–Australian perspective for synthetic inclusions. *Transportation Geotechnics*, **1**(4):171-187. http://dx.doi.org/10.1016/j.trgeo.2014.07.004

Jing, G.Q., 2012. Railway Ballast Bed. China Railway Publishing House, Beijing, China (in Chinese).

Kennedy, J., 2011. A Full-scale Laboratory Investigation into Railway Track Substructure Performance Ballast Reinforcement. PhD Thesis, Heriot-Watt University, Edinburgh, UK.

Kerokoski, O., 2010. Determination of longitudinal and transverse railway track resistance. Joint Rail Conference, p.157-165. http://dx.doi.org/10.1115/JRC2010-36087

Le Pen, L., 2008. Track Behaviour: the Importance of the Sleeper to Ballast Interface. PhD Thesis, University of Southampton, Southampton, UK.

Le Pen, L., Powrie, W., 2011. Contribution of base, crib and shoulder ballast to the lateral sliding resistance of railway track: a geotechnical perspective. *Proceedings of the Institution of Mechanical Engineers, Part F: Journal of Rail and Rapid Transit*, **225**(2):113-128. http://dx.doi.org/10.1177/0954409710397094

Le Pen, L., Bhandari, A.R., Powrie, W., 2014. Sleeper end resistance of ballasted railway tracks. *Journal of Geotechnical and Geoenvironmental Engineering*, **140**(5): 04014004. http://dx.doi.org/10.1061/(asce)GT.1943-5606.0001088

Lim, W.L., 2004. Mechanics of Railway Ballast Behaviour.

PhD Thesis, University of Nottingham, Nottingham, UK.

Mamou, A., Powrie, W., Priest, J.A., *et al*., 2017. The effects of drainage on the behaviour of railway track foundation materials during cyclic loading. *Géotechnique*, **68**(4): 1-10. http://dx.doi.org/10.1680/jgeot.15.P.278

MOR (Ministry of Railways of the People's Republic of China), 2008. Railway Ballast, TB/T 2140-2008. MOR, China (in Chinese).

Nimbalkar, S., Indraratna, B., 2016. Improved performance of ballasted rail track using geosynthetics and rubber shockmat. *Journal of Geotechnical and Geoenvironmental Engineering*, **142**(8):04016031. http://dx.doi.org/10.1061/(asce)GT.1943-5606.0001491

Nurmikolu, A., 2012. Key aspects on the behaviour of the ballast and substructure of a modern railway track: research-based practical observations in Finland. *Journal of Zhejiang University-SCIENCE A (Applied Physics & Engineering)*, **13**(11):825-835. http://dx.doi.org/10.1631/jzus.A12ISGT1

Ruge, P., Birk, C., 2007. Longitudinal forces in continuously welded rails on bridge decks due to nonlinear track bridge interaction. *Computers & Structures*, **85**(7-8):458-475. http://dx.doi.org/10.1016/j.compstruc.2006.09.008

Shi, Y.J., Wang, M., Wang, Y.Q., 2011. Experimental and constitutive model study of structural steel under cyclic loading. *Journal of Constructional Steel Research*, **67**(8): 1185-1197. http://dx.doi.org/10.1016/j.jcsr.2011.02.011

Sung, W., Shih, M., Lin, C., 2005. The critical loading for lateral buckling of continuous welded rail. *Journal of Zhejiang University-SCIENCE*, **6A**(8):878-885. http://dx.doi.org/10.1631/jzus.2005.A0878

UIC (International Union of Railways), 2001. Track/Bridge Interaction Recommendations for Calculations, UIC 774-3E. International Union of Railways, Paris, France.

Wang, Z.G., Jing, G.Q., Yu, Q.F., *et al*., 2015. Analysis of ballast direct shear tests by discrete element method under different normal stress. *Measurement*, **63**:17-24. http://dx.doi.org/10.1016/j.measurement.2014.11.012

Yan, B., Dai, G.L., 2014. Analysis of interaction between continuously-welded rail and high-speed railway bridges considering loading-history. *Journal of the China Railway Society*, **36**(6):75-80 (in Chinese).

Zakeri, J.A., Barati, M., 2015. Utilizing the track panel displacement method for estimating vertical load effects on the lateral resistance of continuously welded railway track. *Proceedings of the Institution of Mechanical Engineers, Part F: Journal of Rail and Rapid Transit*, **229**(3): 262-267. http://dx.doi.org/10.1177/0954409713508937

Zhou, D.P., 1995. Rheological Mechanics and Application in Geotechnical Engineering. Southwest Jiaotong University Press, Chengdu, China (in Chinese).

中文概要

题　目： 散粒体道床在对称位移循环加载下的纵向阻力性能

目　的： 研究散粒体道床在纵向反复荷载下的阻力性能及变化规律是深入理解有砟轨道无缝线路动态服役性能和辨识无缝线路在循环荷载作用下的受力变形机理的基础。本文旨在利用室内足尺试验模型及专用加载系统，分析散粒体道床受循环位移荷载时的纵向阻力性能，探索不同位移加载幅值对有砟道床纵向阻力的影响。

创新点： 1. 利用有砟轨道结构足尺试验模型及循环加载装置，测试循环荷载下的道床纵向阻力-位移滞回曲线；2. 根据循环加载试验曲线，构建滞回模型，刻划散粒体道床的纵向承载和传力性能。

方　法： 1. 通过试验分析，得到散粒体道床在周期性荷载作用下的力-位移曲线（图 6、8 和 10）； 2. 基于试验数据，分析散粒体道床在周期性荷载下的滞回准则，得到不同位移幅值下滞回曲线的演化规律（图 7、9 和 11）；3. 通过图像识别技术，对周期性荷载作用下道砟颗粒的运动规律进行分析，从散粒体道床的细观作用机理分析宏观力学表现（图 16~18）。

结　论： 1. 散粒体道床在循环往复荷载下的纵向阻力-位移曲线为一条封闭的滞回曲线，且存在明显的耗能现象；2. 在位移幅值保持不变的循环过程中，散粒体道床表现出一种循环软化行为；3. 位移幅值不同，道床纵向阻力的衰减率不同，且位移越大，退化效应越明显。

关键词： 散粒体道床；位移幅值；循环加载；纵向阻力